A Movable-Mass Attitude-Stabilization System for Artificial-g Space Stations

DARA W. CHILDS*
Colorado State University, Fort Collins, Colo.

The development of an active, momentum-exchange system to be used for attitude stabilization of a class of artificial-g spaces stations configurations is studied. A system which employs a single movable control mass is considered for the control of a space station which has the physical appearance of two rigid bodies connected by a long and comparatively slender structure. Both the physical arrangement for a stabilizer and requisite control laws are presented. The exceptional effectiveness of the system proposed in stabilizing the space station is explained both analytically, and in terms of analog simulation results. The analog results illustrate the significant parameters of the control logic, normal and overload behavior of the stabilizer, and the effect of control force limitation. The influence of structural dynamics on control system performance and the adaptation of the controller for an attitude-hold mode are also discussed. Current space station inertia properties and the expected disturbance levels require a system of approximately 500 lb total Earth weight (250,000 lb space station). The control logic developed is extremely simple, and requires a low maximum force level on the order of 30 lb.

Introduction

THE objectives of the U. S. space program for the seventies include the development of a manned space station. A basic objective is a station which can be converted either from zero-g to artificial-g operations or vice versa. During the zero-g mode, attitude will be maintained by a combined Control Moment Gyro (CMG) and thruster attitude control system in a fashion similar to that planned for the Sky-Lab program[1]; however, the requirements for attitude control and the means for supplying it in the artificial-g mode remain unresolved.

Space station pointing requirements in the artificial-g mode are ultimately dictated by the power source design. If solar arrays are used, one must obviously have sun-pointing capability. However, if a nuclear power source is provided, a random orientation may be acceptable with no attendant pointing requirements. In either case, a significant portion of the attitude-control systems' responsibility is attitude stabilization or, what is commonly referred to as wobble damping. A space station is said to be "wobbling" when its axis of maximum moment of inertia is not aligned with its moment-of-momentum vector.

Ideally, the attitude-stabilization systems in both the artificial-g and zero-g modes would use the same torqueing devices. The major impediment to this approach with respect to CMG's is the marked increase in CMG gimbal loading in the artificial-g mode. The maximum CMG gimbal angle (from the space station spin axis) must be reduced in the artificial-g mode to prevent gimbal failures.[2] In short, either the gimbals must be strengthened or the CMG's operated at less than peak efficiency (with respect to their momentum capability). A material improvement in CMG lifetime and design, as well as a reduction in power consumption can be achieved if the CMG system can simply be "turned off" during the artificial-g mode.

The alternatives for artificial-g attitude stabilization are a) reaction-jet control, b) passive wobble dampers, c) active wobble dampers, or d) momentum wheels used as dampers. The use of reaction jets for wobble damping is unrealistic from a fuel viewpoint, while a momentum wheel would have

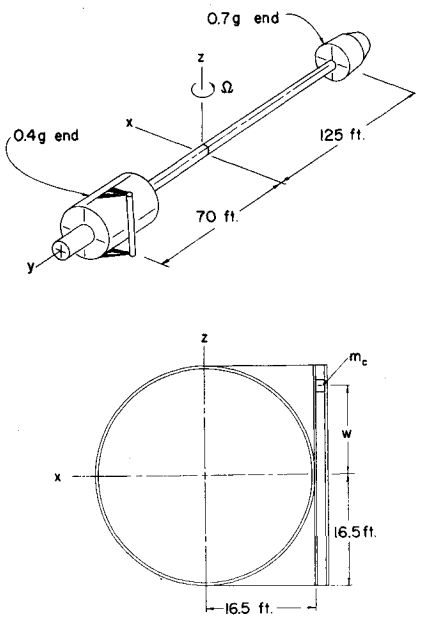

Fig. 1 Artificial-g space station and stabilizer configuration.

Received October 15, 1970; revision received May 26, 1971. This work was performed while the author was a participant in the 1970 NASA-ASEE Summer Faculty Fellowship Aeronautics and Space Research Program, Marshall Space Flight Center, Huntsville, Ala. The NASA associate in this program was H. E. Worley, and his valuable suggestions are gratefully acknowledged. Publication of this paper is made possible through NASA contract NAS8-27440. This support is gratefully acknowledged

Index Category: Manned Space Station Systems; Spacecraft Attitude Dynamics and Control.

* Assistant Professor of Mechanical Engineering; presently Associate Professor of Applied Mathematics and Mechanical Engineering, Speed Scientific School, the University of Louisville, Louisville, Ky. Associate Member AIAA.

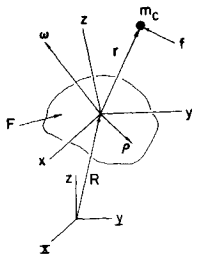

Fig. 2 Kinematic variables for the derivation of general equations of motion.

substantially the same problems as a CMG system. Taylor[3] has indicated that a passive pendulum system is feasible for some space station configurations, and such a system has evident advantages with respect to reliability, simplicity, etc.

The system developed and advocated in this study makes use of a single, movable mass to affect control. It is, in a sense, an active version of prior[4] passive dampers, but it also acts as a "mass-balancer"[5] to minimize the "felt" disturbances acting on the system. By incorporating both "mass-balancing" and damping, the controller achieves critical wobble damping rates. Comparisons of the system developed in this study with Taylor's[3] passive system are difficult because of the differences in space station configurations; however, the system of this paper constitutes 0.2% of space station weight as compared to 1.5% for Taylor's system.

Uncontrolled Space Station Dynamic Model

Figure 1 (top) illustrates the general type of space station configuration considered in this study for artificial-g operations, namely, two bodies connected by a comparatively light structure. The rotational motion of this system about a transverse axis (of maximum moment of inertia) through the mass center yields a "usable" artificial-g field at one or both ends of the system. The system considered in this study has the following nominal inertia properties

$$I_{\bar{z}} = 51.03 \times 10^6 \text{ slug-ft}^2, \quad I_{\bar{x}} = 50.90 \times 10^6 \text{ slug-ft}^2 \tag{1}$$

$$I_{\bar{y}} = 1.07 \times 10^6 \text{ slug-ft}^2, \quad M = 8{,}250 \text{ slugs}$$

and has a nominal spinrate of $\Omega = 4$ rpm.

As stated previously, wobbling occurs when the H (moment-of-momentum) vector and the $\bar{z}$ axis (axis of maximum moment-of-inertia) do not coincide. We are concerned in this study with removing the wobble which results from crew-motion disturbances that force **H** and $\bar{z}$ apart. The reference "worst-case" disturbance used herein consists of four astronauts (773 lb or 24 slugs) displaced instantaneously to the worst possible coordinate locations within the spacecraft, i.e., the system is designed to handle the step product-of-inertia disturbances

$$I_{xz}(0) = 3250 \text{ slug-ft}^2, \quad I_{yz}(0) = 49{,}700 \text{ slug-ft}^2 \tag{2}$$

These values result from the particular geometry of the configuration examined.

The effect that such a disturbance has on the system can be explained as follows. Illustrated in Fig. 1 is an x,y,z coordinate system which is, by definition, fixed in the space station. The origin of this system coincides with the mass center of the space station, and the system itself nominally coincides with the $\bar{x},\bar{y},\bar{z}$ principal axis system, where $\bar{z}$ is the maximum moment-of-inertia axis. If these two coordinate systems initially coincide, an instantaneous mass disturbance yields

$$\begin{aligned} I_{xz} &= m_d x_d z_d = -\beta(I_{\bar{z}} - I_{\bar{x}}) \\ I_{xy} &= m_d x_d y_d = -\gamma(I_{\bar{x}} - I_{\bar{y}}) \\ I_{yz} &= m_d y_d z_d = \alpha(I_{\bar{z}} - I_{\bar{y}}) \end{aligned} \tag{3}$$

where the (small) angles α,β,γ define the misalignment between the x,y,z and $\bar{x},\bar{y},\bar{z}$ axes, respectively. I_{xy} disturbances, with their "in plane" γ misalignments, have no effect on the artificial-g environment or the $\bar{z}$ axis and are not considered here.

Accordingly, only I_{xz} and I_{yz} are of interest, and the angles (α,β) provide a measure of their potential for exciting wobble. This statement is clarified by examining the infinitesimal, constant, coordinate transformation

$$\begin{Bmatrix} V_{\bar{x}} \\ V_{\bar{y}} \\ V_{\bar{z}} \end{Bmatrix} = \begin{bmatrix} 1 & 0 & -\beta \\ 0 & 1 & \alpha \\ \beta & -\alpha & 1 \end{bmatrix} \begin{Bmatrix} V_x \\ V_y \\ V_z \end{Bmatrix} \tag{4}$$

defined in terms of the components of the arbitrary vector **V** in the $\bar{x},\bar{y},\bar{z}$ and x,y,z systems. Suppose the angular-velocity vector of the system prior to the disturbance is defined by $\omega_z = \Omega, \omega_x = \omega_y = 0$. Then from Eq. (4), the initial conditions following the (instantaneous) disturbance are

$$\omega_{\bar{x}}(0) = -\beta\Omega, \quad \omega_{\bar{y}}(0) = \alpha\Omega, \quad \omega_{\bar{z}}(0) = \Omega \tag{5}$$

These initial conditions can be numerically evaluated from Eqs. (1) and (2) to be

$$\begin{aligned} \alpha_{\max} &= 0.057^\circ = 0.994 \times 10^{-3} \text{ rad} \\ \beta_{\max} &= 1.29^\circ = 2.25 \times 10^{-2} \text{ rad} \end{aligned} \tag{6}$$

which indicates that I_{xz} is the more potent sources of wobble excitation.

The general solution to Euler's equations of motion for the body rates $\omega_{\bar{x}}(t)$, $\omega_{\bar{y}}(t)$, $\omega_{\bar{z}}(t)$ in terms of elliptic integrals is well known[6]; however, for the present study an accurate approximate solution can be obtained by noting from Eqs. (5) and (6) that both $\omega_{\bar{x}}$ and $\omega_{\bar{y}}$ are much smaller than $\omega_{\bar{z}}$. This property of the motion allows one to assume that the spin velocity is constant, i.e., $\omega_{\bar{z}}(t) = \omega_{\bar{z}}(0) = \Omega$.† Accordingly, the equations of motion can be stated as

$$\begin{aligned} \dot{\omega}_{\bar{x}} + a\Omega\omega_{\bar{y}} = 0, \quad \dot{\omega}_{\bar{y}} - b\Omega\omega_{\bar{x}} = 0, \\ \omega_{\bar{z}}(t) = \omega_{\bar{z}}(0) = \Omega \end{aligned} \tag{7}$$

where

$$a = (I_{\bar{z}} - I_{\bar{y}})/I_{\bar{x}}, \quad b = (I_{\bar{z}} - I_{\bar{x}})/I_{\bar{y}} \tag{8}$$

The solution to Eq. (7) for the initial conditions of Eq. (5) is

$$\begin{aligned} \omega_{\bar{x}}/\Omega &= -\beta \cos\lambda\Omega t - (a\alpha/\lambda) \sin\lambda\Omega t \\ \omega_{\bar{y}}/\Omega &= \alpha \cos\lambda\Omega t - (b\beta/\lambda) \sin\lambda\Omega t \end{aligned} \tag{9}$$

where

$$\lambda\Omega = (ab)^{1/2}\Omega = 0.0225 \text{ cps} \tag{10}$$

Differences between the approximate solution of Eq. (9) and the exact solution[6] are of the same order as that cited for $\omega_{\bar{z}}(t)$.

By using the inverse transformation defined from Eq. (4), the body-fixed angular velocity components $\omega_x(t),\omega_y(t),\omega_z(t)$ can be obtained from the solutions of Eqs. (9) and (7). The alternative model used in this study to define uncontrolled space station motion is

$$\begin{aligned} \dot{\omega}_x + a\Omega\omega_y &= -\Omega^2 I_{yz}(0)/I_x = -\Omega^2 a\alpha(0) \\ \dot{\omega}_y - b\Omega\omega_x &= \Omega^2 I_{xz}(0)/I_y = -\Omega^2 b\alpha(0) \\ \omega_z(t) &= \Omega, \quad \omega_x(0) = \omega_y(0) = 0 \end{aligned} \tag{11}$$

The solution for ω_x and ω_y from Eq. (11) coincides with the approach just cited, and the error in $\omega_z(t)/\Omega$ is on the order of β^2. In terms of this model, the control problem can be summarized as follows: Devise a feedback control system

† A numerical evaluation of the exact solution yields $\max|\omega_{\bar{z}}(t) - \Omega|/\Omega = 2.5 \times 10^{-4}$.

(configuration and logic) which will efficiently realize the final state

$$\dot{\omega}_x(t_f) = \dot{\omega}_y(t_f) = 0 \tag{12}$$

for the expected initial conditions and worst case disturbances.

Total System Model

Figure 1 illustrates the physical arrangement of a system which is designed to minimize and remove the wobble motion caused by product of inertia disturbances. As illustrated, the essential element of the stabilizer is a rigid body of mass m_c whose motion is limited by a tube (or other physical constraints) to be parallel with the z axis. The position of the mass within the tube is defined by the variable w. In this section, the exact equations of motion for the space station-controller system will be derived, and an approximate linear model based on these equations will be justified.

Figure 2 illustrates the pertinent dynamic variables required to define the equations of motion. The resultant external force applied to the system is $\mathbf{F}$, and $\mathbf{T}$ is the resultant external torque applied to the system at the origin of the body fixed x,y,z system. The force $\mathbf{f}$ is the net force acting on m_c. The vector $\mathbf{R}$ locates the origin of the x,y,z (body-fixed) system in the X,Y,Z (inertial system), the vector $\mathbf{r}$ locates the control mass m_c in the x,y,z system, and the vector $\boldsymbol{\varrho}$ is the position vector in the x,y,z system. The angular-velocity vector of the x,y,z system is identified by $\boldsymbol{\omega}$.

From Newtons' laws of motion the basic defining equations for the system may be stated as

$$\mathbf{F} = \int_M (\ddot{\mathbf{R}} + \ddot{\boldsymbol{\varrho}})dm + m_c(\ddot{\mathbf{R}} + \ddot{\mathbf{r}}) \tag{13}$$

$$\mathbf{T} - \mathbf{r} \times \mathbf{f} = \int_M \boldsymbol{\varrho} \times (\ddot{\mathbf{R}} + \ddot{\boldsymbol{\varrho}})dm \tag{14}$$

$$\mathbf{f} = m_c(\ddot{\mathbf{R}} + \ddot{\mathbf{r}}) \tag{15}$$

where M is the mass of the rigid body, and the operation $\dot{\mathbf{V}}$ implies time differentiation with respect to the X,Y,Z system. The origin of the x,y,z system is defined to coincide with the mass center of the rigid body; hence,

$$\int_M \boldsymbol{\varrho} dm = 0 \tag{16}$$

Suitable kinematic definitions for $\ddot{\mathbf{r}}$ and $\ddot{\boldsymbol{\varrho}}$ are

$$\ddot{\mathbf{r}} = \hat{\ddot{\mathbf{r}}} + 2\boldsymbol{\omega} \times \hat{\dot{\mathbf{r}}} + \dot{\boldsymbol{\omega}} \times \mathbf{r} + \boldsymbol{\omega} \times (\boldsymbol{\omega} \times \mathbf{r}) \tag{17}$$

$$\ddot{\boldsymbol{\varrho}} = \dot{\boldsymbol{\omega}} \times \boldsymbol{\varrho} + \boldsymbol{\omega} \times (\dot{\boldsymbol{\omega}} \times \boldsymbol{\varrho}) \tag{18}$$

where the operation $\hat{\mathbf{V}}$ implies time differentiation with respect to the x,y,z system. Substitution from Eqs. (16) and (18) into Eq. (13) yields

$$\mathbf{F} = (M + m_c)\ddot{\mathbf{R}} + m_c\ddot{\mathbf{r}} \tag{19}$$

The space stations considered in this study are assumed to be in a circular orbit such that the gravitational forces and the inertial forces due to radial acceleration are in equilibrium. The effect of either disturbance or control mass motion on spacestation dynamics is of interest. If the essentially constant and equal radial acceleration and gravity terms are cancelled in Eq. (19), $\delta\ddot{\mathbf{R}}$ (the acceleration of the space station-mass system due to control-mass motion) is defined by

$$\delta\ddot{\mathbf{R}} = -\{m_c/(M + m_c)\}\ddot{\mathbf{r}} = -\epsilon\ddot{\mathbf{r}} \tag{20}$$

Due to the relative magnitudes of m_c and M, ϵ is on the order of 10^{-3}. Cancelling the gravitational and radial acceleration terms in Eq. (15) yields from Eq. (20)

$$\tilde{\mathbf{f}} = m_c\ddot{\mathbf{r}}(1 - \epsilon) \cong m_c\ddot{\mathbf{r}} \tag{21}$$

where $\tilde{\mathbf{f}}$ is the reaction force applied to the control mass and reacted by the space station. Note that no approximation is involved in arriving at either Eq. (20) or the first of (21). Hence, the conclusion to be drawn from Eq. (21) is that the effect of system mass center migration relative to the space station on control dynamics would be the same as that resulting from a 0.1% error in control mass computation, viz., negligible.

From Eq. (17), the component definition for Eq. (21) is

$$\tilde{f}_x = m_c\{2\omega_y\dot{w} + \dot{\omega}_y w - \dot{\omega}_z r_y + \omega_x\omega_z w + \omega_x\omega_y r_y - r_x(\omega_z^2 + \omega_y^2)\} \tag{22a}$$

$$\tilde{f}_y = m_c\{-2\omega_x\dot{w} - \dot{\omega}_x w + \dot{\omega}_z r_x + \omega_y\omega_x r_x + \omega_y\omega_z w - r_y(\omega_z^2 + \omega_x^2)\} \tag{22b}$$

$$\tilde{f}_z = m_c\{\ddot{w} + r_y\dot{\omega}_x - r_x\dot{\omega}_y + \omega_x\omega_z r_x + \omega_y\omega_z r_y - w(\omega_x^2 + \omega_y^2)\} \tag{22c}$$

where (r_x,r_y,w) are the components of $\mathbf{r}$ in the x,y,z system.

Equation (14) can be reduced in an analogous fashion by a) eliminating the gravity-gradient torque, b) substituting from Eq. (18) and the vector identity $\mathbf{A} \times [\mathbf{B} \times (\mathbf{B} \times \mathbf{A})] = \mathbf{B} \times [\mathbf{A} \times (\mathbf{B} \times \mathbf{A})]$, and c) performing the indicated integrations. The result is the matrix equation.

$$-[(r)](\tilde{f}) = [J](\dot{\omega}) + [(\omega)][J](\omega) \tag{23}$$

stated in the x,y,z system where $[J]$ is the inertia matrix of the space station, and the notation $[(V)]$ implies

$$[(V)] = \begin{bmatrix} 0 & -V_z & V_y \\ V_z & 0 & -V_x \\ -V_y & V_x & 0 \end{bmatrix}$$

and performs the matrix equivalent of the vector-cross-product operation. The desired format for Eq. (23) is obtained by a) replacing $\tilde{f}_x$ and $\tilde{f}_y$ by their definitions in Eq. (22), b) implementing the assumptions of the preceding section ($\omega_z = \Omega$, $\dot{\omega}_z \cong 0$, $\omega_x/\Omega \ll 1$, $\omega_y/\Omega \ll 1$), and c) noting that $m_c w^2/I_x \ll 1$ and $m_c w^2/I_y \ll 1$. The resulting equations are

$$I_x\dot{\omega}_x + (I_z - I_y)\Omega\omega_y + 2m_c w\dot{w}\omega_x + I_{yz}(t)\Omega^2 = -r_y\tilde{f}_z$$

$$I_y\dot{\omega}_y - (I_z - I_x)\Omega\omega_x + 2m_c w\dot{w}\omega_y - I_{xz}(t)\Omega^2 = r_x\tilde{f}_z \tag{24}$$

where

$$I_{xz}(t) = I_{xz}(0) + m_c r_x w, \quad I_{yz}(t) = I_{yz}(0) + m_c r_y w \tag{25}$$

Furthermore, the "Coriolis-torque" terms $2m_c w\dot{w}\omega_x$ and $2m_c w\dot{w}\omega_y$ are quite small. Specifically, the conservative assumptions ($\dot{w} = 5$ fps, $\omega_x = \beta\Omega$, $\omega_y = \alpha\Omega$, $w = 16.5$ ft) yields resultant torques of $2m_c w\dot{w}\omega_x \cong 17.2$ ft-lb and $2m_c w\dot{w}\omega_y \cong 0.74$ ft-lb. The effect of transient torques of this magnitude are insignificant for the system under consideration. The final system equations are

$$\dot{\omega}_x + a\Omega\omega_y = -(r_y/I_x)\tilde{f}_z - \Omega^2 I_{yz}(t)/I_x$$

$$\dot{\omega}_y - b\Omega\omega_x = (r_x/I_y)\tilde{f}_z + \Omega^2 I_{xz}(t)/I_y \tag{26}$$

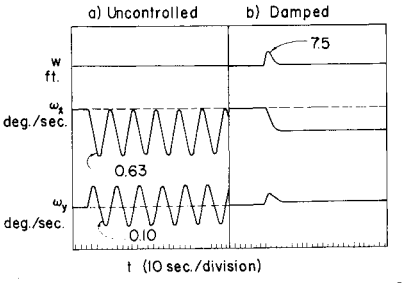

Fig. 3 Wobble motion for $I_{xz}(0) = 1400$ slug-ft^2 with a) no control, and b) wobble damper on, for $k_2 = 25$ lb/ft, $k_2 = 2.5 \times 10^5$ lb-sec/rad, and $k_3 = 0.25$ lb/ft-sec.

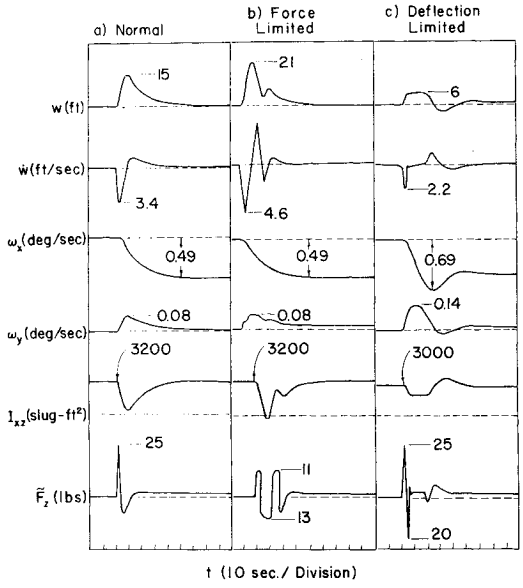

Fig. 4 Wobble damper performance for a) normal control, b) force limited control, and c) deflection limited control. For all cases k_1 = 25 lb/ft, k_2 = 2.5 × 10^5 lb-sec/rad, and k_3 = 0.25 lb/ft-sec.

and

$$\ddot{w} = \tilde{f}_z(t)/m_c + (r_x\dot{\omega}_y - r_y\dot{\omega}_x) - \Omega(r_x\omega_x + r_y\omega_y) \quad (27)$$

It is convenient to separate the net force applied to the system into a control force $u(t)$ and the balance of the physical forces (motion stops, coulomb damping, etc.) $v(t)$, i.e., $\tilde{f}_z(t) = u(t) + v(t)$.

Control Formulation

The effectiveness of the movable-mass controller defined by Eq. (25-27) as a wobble damper is based on the following two observations: 1) The dominant term on the right of Eq. (26) is $\bar{\Omega}^2 I_{xz}(t)/I_y$, and 2) $I_{xz}(t)$, as defined in Eq. (25), may be easily and rapidly controlled. A simple and effective control logic based on these observations simply forces w [and hence $-I_{xz}(t)$] to be proportional to ω_y. The feedback control logic which brings this about is

$$u = -k_1 w + k_2\omega_y \quad (28)$$

For reasonable values of the "spring constant" k_1, the control mass behaves like a simple harmonic oscillator. For sufficiently large values of k_1, the natural frequency of this system $(k_1/m_c)^{1/2}$ is well above the input wobble frequency $\lambda\Omega$, and as a result

$$w \cong (k_2/k_1)\omega_y = c\omega_y \quad (29)$$

Since the $\tilde{f}_z(t)$ terms in Eq. (26) are generally small in comparison to the product-of-inertia terms, one obtains from Eqs. (26, 25, and 29)

$$\ddot{\omega}_y + cm_c|r_x|I_y^{-1}\Omega^2\dot{\omega}_y + (a + \delta a)b\Omega^2\omega_y = -b\Omega^3 I_{yz}(0)I_x^{-1} \quad (30)$$

where

$$\delta a = c\Omega m_c|r_y|I_x^{-1}, \quad r_x = -|r_x|, \quad r_y = |r_y| \quad (31)$$

The conclusion to be drawn from Eqs. (30) and (31) is that a control logic of the form Eq. (28) which results in the satisfaction of Eq. (29) will provide wobble damping, and that the rate of damping is proportional to the parameter c. The ratio of effective damping to critical damping is defined from

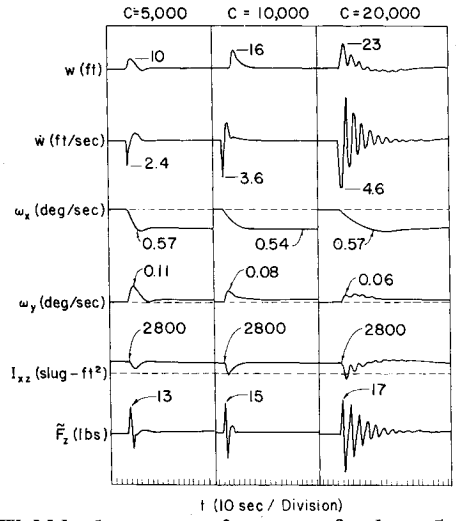

Fig. 5 Wobble damper performance for k_2 = 5 × 10^4 lb-sec/rad, k_3 = 0.25 lb/ft-sec, and a) k_1 = 10 lb/ft, b) k_1 = 5 lb/ft, c) k_1 = 2.5 lb/ft.

Eq. (30) by

$$\zeta = cm_c|r_x|\Omega/2I_y\lambda \quad (32)$$

One also notes that the controller increases the wobble natural frequency via the δa term; however, this is not generally significant. Although the control analysis cited above is quite simple, it is conclusively verified by the simulation results which follow.

Simulation Results

The significance of the terms in the control function (28) are most easily explained in terms of the analog simulations which follow. In addition to Eq. (1) and Eq. (2), the parameters used in this study to define the physical system are

$$r_x = -16.5 \text{ ft}, \; r_y = 42.3 \text{ ft}, \; m_c = 11 \text{ slugs} \quad (33)$$

The control mass was "sized" by assuming the physical limitation

$$|w| \leq 16.5 \text{ ft} \quad (34)$$

and requiring that the static I_{xz} control capability match the maximum expected disturbance values given in Eq. (2). From Eqs. (25, 33, and 34) the resultant *static* control capability is $I_{xz}{}^c \cong 3000$ slug-ft², and $|I_{yz}{}^c| \cong 7700$ slug-ft². The equivalent static torque capability is $|T_x|_{\max} \cong 1350$ ft-lb, and $|T_y|_{\max} \cong 525$ ft-lb.

The effectiveness of the control function given in Eq. (28) is best appreciated by an examination of Fig. 3 which illustrates system response to a step product-of-inertia disturbance [$I_{xz}(0)$ = 1400 slug-ft²] with and without control. As can be seen, the wobble damper virtually eliminates the disturbance. The remarkably effective control illustrated in Fig. 3b is the result of two physical effects. Not only does the term $k_2\omega_y$ in Eq. (28) result in the linear damping suggested by Eq. (30), it also yields a reduction in the disturbance "felt" by the space station. This is illustrated in Fig. 4a where one notes that $I_{xz}(t)$ is rapidly reduced by the change in w. The term $-k_1 w$ in Eq. (28) tends to reduce the change in w caused by the disturbance and is primarily responsible for the (comparatively) slow return of w to zero and $I_{xz}(t)$ to $I_{xz}(0)$. It is primarily during this "retraction" phase of the control cycle that the wobble motion is removed. Since [Eq. (20)] the final value for ω_y is not zero, the term $-k_1 w$ in Eq. (28) will not return w to zero, and the complete control function employed was

$$u = -k_1 w + k_2\omega_y - k_3\int_0^t w(\phi)d\phi \quad (35)$$

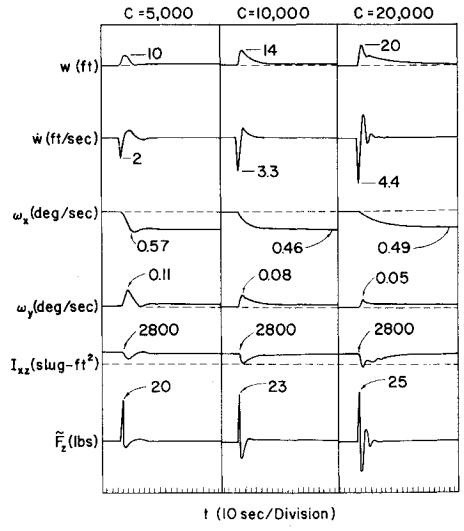

Fig. 6 Wobble damper performance for $k_2 = 2.5 \times 10^5$ lb-sec/rad, $k_3 = 0.25$ lb/ft-sec, and a) $k_1 = 50$ lb/ft, b) k_1, = 25 lb/ft, c) $k_1 = 12.5$ lb/ft.

The control mass is returned to its neutral position ($w = 0$) in order to restore its full control potential. The additional integral term has no other effect on control dynamics.

The differences between a mass-balancing control objective[5] and the wobble-damping objective satisfied by Eq. (35) are as follows. A mass balancing controller would be employed to force, and hold, $I_{xz}(t)$ to zero. However, as can be seen in Fig. 4a, the wobble-damping control law cited in Eq. (35) causes a rapid reduction of $I_{xz}(t)$ followed by its gradual restoration to $I_{xz}(0)$.

Figures 5 and 6 illustrate the changes in control-system response associated with changes in the gain constant k_1 and k_2 and their ratio $c = k_2/k_1$. In each of the two figures, k_2 is held constant, while k_1 is reduced such that equal values of c result. As can be seen, $c = 10{,}000$ (ft-sec/rad) yields the appearance of critical damping in the wobble components ω_x and ω_y, while $c = 5000$ and $c = 20{,}000$ result in underdamped and overdamped responses, respectively. This would be expected, since for the system considered critical damping is predicted from Eq. (32) for $c \cong 9500$. One notes that the peak force levels are increased by increasing the value of k_2, and decreased by increasing k_1. The oscillations in w which are most evident in Fig. 5a are the result of small values for the parameter k_1; however, one notes that these oscillations have little effect on the wobble-damping rates. Further, the peak values for w are largely a function of c, and can be considerably reduced if less than critical damping is acceptable, e.g., in Fig. 6a, $w(\max) = 10$ ft for $I_{xz}(0) = 2800$ slug-ft^2. Hence, in this case, a disturbance of approximately 4600 slug-ft^2 would be required to saturate the controller ($w = 16.5$ ft). The two basic conclusions to be drawn from Figs. 5 and 6 are the following: 1) critical wobble damping can be easily obtained, and 2) the control logic is relatively insensitive to parametric variations.

One notes in the (c) portions of Figs. 5 and 6 that the peak values of w violate the physical constraint cited in Eq. (34). Figure 4c illustrates what happens when a physical contraint on the mass motion is enforced. For the case illustrated, the normal peak value of w would be 14 ft; however, its deflection is physically limited (in the case shown) by $|w| \leq 6$ ft. A comparison of (a) and (c) of Fig. 4 reveals that saturation does not seriously degrade the damper's performance. Figure 4b illustrates the consequence of limiting the control force u as follows; -13 lb $\leq u \leq 11$ lb. A comparison of (a) and (b) in Fig. 4 shows that this also does not materially reduce the damping of ω_x and ω_y.

Although the system developed and discussed herein is designed to provide wobble damping without pointing capability, it can be modified to act as a "mass balancer" and provide some attitude hold capability. Suppose that the control objective for some phase of the mission consisted of the requirement that the z (body-axis) and the angular momentum vector **H** be maintained in alignment while subjected to crew-motion disturbances. The control law

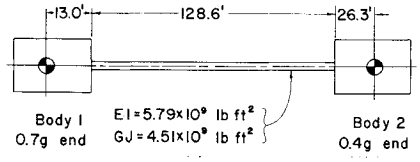

Fig. 7 Structural dynamics model.

$$u = -k_1 w + k_2 \omega_y - k_4 \omega_x - k_5 \int_0^t \omega_x(\phi) d\phi$$

will cause $\omega_x(t)$ and hence $\beta(t)$ to be forced and held to zero. Since this control law does not affect the final value of α, it can only hold the separation of **H** and z to within α degrees. However, from Eq. (6) this results in a significant pointing error reduction.

The possibility that structural dynamics of the space station might degrade the performance of the attitude-stabilization system was investigated. The idealized structural dynamics model employed is illustrated in Fig. 7, and consists of two rigid bodies connected by a massless beam. All of the space station inertia was concentrated in the two bodies. The torsional moments of inertia for bodies 1 and 2 are $I_{y1} = 0.30$ slug-ft^2, $I_{y2} = 0.77$ slug-ft^2, and the fundamental torsional frequency is defined by

$$\Omega_T = \{k_t(I_{y1} + I_{y2})/I_{y1}I_{y2}\}^{1/2} = 1.66 \text{ cps}$$

where $k_t = GJ/l = 0.234 \times 10^8$ ft-lb/rad. The computed torsional frequency is more than 70 times greater than the wobble frequency $\lambda\Omega = 0.0225$ cps. The masses of the two rigid bodies of Fig. 7 were $m_1 = 2.30 \times 10^3$ slugs and $m_2 = 5.95 \times 10^3$ slugs. The moments of inertia for spin-plane bending were $I_{x1} = 1.52 \times 10^6$ slug-ft^2 and $I_{x2} = 5.95 \times 10^6$ slug-ft^2, while for out-of-plane bending the parameters were $I_{x1} = 1.48 \times 10^6$ slug-ft^2 and $I_{x2} = 4.81 \times 10^6$ slug-ft^2. Modal analysis of the systems defined by these parameters had the following results. The first spin-plane bending mode was $\Omega_{bz} = 0.72$ cps, and the first out-of-plane bending mode was $\Omega_{bx} = 0.71$ cps. These frequencies are approximately thirty times greater than $\lambda\Omega$.

A simulation model based on Likins[7] and Childs[8] analyses which included the torsional and out-of-plane bending modes indicated that due to the wide frequency separations cited above there is little or no interaction between rigid-body and structural dynamics. However, the simulation revealed that the control system could "tune" with the bending or torsional modes, and indicated that sensor signals should be filtered to remove the structural dynamic contribution. Because of the large separation between the frequencies involved, such filtering was easily accomplished. The following precautionary note is injected with respect to torsional structural dynamics. The torsional frequency computed ($\Omega_T = 1.66$ cps) holds for a telescoping-tunnel connecting member. If cables were used for this member, the torsional rigidity would be virtually nil, and control would have to be provided for structural as well as rigid body dynamics.

Conclusions

A movable mass controller of the type discussed herein provides a viable, practical, and attractive means for artificial-g space station stabilization. It has the following desirable attributes:

1) Light Weight. The system cited herein with a control mass of 11 slugs or 352 lb could have a total launch weight of approximately 500 lb.

2) Simplicity. The control logic cited in Eq. (28) is extremely simple, and the results of this study indicate that the servomechanism requirements for implementation of the system are modest, both in terms of peak force and frequency response requirements. Sensor requirements are also modest, since only w and ω_y must be measured. The implementation of this system would be considerably simpler than competitive systems such as fluid-displacement systems, movable mass on boom arrangements, inertia wheels, CMG's, etc.

3) Power Requirements. The low level of peak and sustained force levels required for the controller indicates a quite low level of power consumption. A movable mass controller has a significant advantage, in this respect, over CMG's or inertia wheels.

References

[1] "ATM Pointing Control System (PCS) Astronaut Operations Requirements Document (AORD)," 50M37934, March 1969, NASA.

[2] Senator, F. E. et al., Skylab "B" Workshop Systems Engineering and Program Definition, MDC G0447, July 1970, McDonnell Douglas Astronautics Company-West.

[3] Taylor, R. S., "A Passive Pendulum Wobble Damping System for a Manned Rotating Space Station," *Journal of Spacecraft and Rockets*, Vol. 3, No. 8, Aug. 1966, pp. 1221–1228.

[4] Meirovitch, L. and Nelson, H. D., "On the High-Spin Motion of a Satellite Containing Elastic Parts," *Journal of Spacecraft and Rockets*, Vol. 3, No. 11, Nov. 1966, pp. 1597–1602.

[5] Sunkel, J. W., "Study of Space Base Balance Control Techniques," NASA Internal Note, MSC-EG-70-11, March 1970, Manned Spacecraft Center, Houston, Texas.

[6] Arnold, R. N. and Maunder, L., *Gyrodynamics and Its Engineering Applications*, Academic Press, New York, 1961.

[7] Likins, P. W., "Modal Method for Analysis of Free Rotations of Spacecraft," *AIAA Journal*, Vol. 5, No. 1, July 1967, pp. 1304–1308.

[8] Childs, D. W., "Simulation Models for Flexible Spinning Bodies," *SIMULATION*, June 1969, pp. 291–296.

AUGUST 1971 J. SPACECRAFT VOL. 8, NO. 8

Attitude Stabilization of Synchronous Communications Satellites Employing Narrow-Beam Antennas

H. J. Dougherty,* K. L. Lebsock,† and J. J. Rodden‡
Lockheed Missiles & Space Company, Sunnyvale, Calif.

Future communications satellites will employ multiple narrow-beam antennas covering widely separated areas of the Earth. Some of these narrow beams must cover more than one ground station, necessitating coverage of stations located at the fringes of the antenna beams. This imposes a requirement for high pointing accuracies; current estimates for satellites to be put into service in 1972 and beyond being for beam pointing accuracies of 0.1° or less. An additional requirement for future satellites will be longer life-times; operating lives of 10 yr are presently being considered. Attitude stabilization systems using momentum and reaction wheels in various combinations are evaluated based on these requirements. The candidate wheel stabilization systems are discussed in terms of their respective design parameters and performance characteristics. Comparisons are made between the systems on the basis of wheel size, weight, and power required to achieve high pointing accuracies.

Nomenclature

B = antenna beam width
E = antenna elevation angle in radians
H_z = yaw wheel momentum
h = angular momentum of pitch wheel
h_R = required control momentum
I_x, I_y, I_z = principal moments of inertia
K = autopilot gain
$K_{\dot\theta}, K_\theta, K_I$ = controller rate, position and integral gain, respectively
K_D = desaturation gain
k = factor relating required momentum to peak disturbance torque, or ratio of yaw gain to roll gain
M_{xc}, M_{zc} = control moments about roll and yaw axes, respectively
N = correction factor
n = number of days between momentum desaturation
P_P, P_A = peak and average power, respectively
P_m, P_R = momentum wheel power and three-axis reaction wheel system power, respectively
s = Laplace operator
T_c = cyclic disturbance torque
T_M, T_{MP} = motor torque for disturbances and peak motor torque, respectively
T_p = peak disturbance torque
T_S = inertial fixed disturbance torque
T_x, T_z = disturbance torques about roll and yaw axes, respectively
W = weight of momentum control system
α = offset angle of roll-yaw coupled control thruster
ϵ = attitude pointing error
ϕ = roll angle
ψ = yaw angle
θ = pitch angle
τ = lead time constant in control system
τ_m = motor time constant
τ_z = nonminimum phase zero time constant
ω_0 = orbital rate, 7.29×10^{-5} rad/sec for synchronous orbit

Presented as Paper 70-457 at the AIAA 3rd Communications Satellite Systems Conference, Los Angeles, Calif. April 6–8, 1970; submitted October 16, 1970; revision received February 22, 1971. The results in this paper are based on studies performed under Lockheed's Independent Development Program and COMSAT Corporation Contract CSC-SS-202.

* Staff Engineer, Attitude Stability and Control Systems, Department 62-11. Member AIAA.

† Scientist Associate, Attitude Stability and Control Systems, Department 62-11.

‡ Manager, Attitude Stability and Controls Systems, Department 62-11. Member AIAA.